Coordination Chemistry Reviews
196 (2000) 31–63

COORDINATION CHEMISTRY REVIEWS

www.elsevier.com/locate/ccr

The interaction of metal oxide surfaces with complexing agents dissolved in water

M.A. Blesa *, A.D. Weisz, P.J. Morando, J.A. Salfity, G.E. Magaz, A.E. Regazzoni

Unidad de Actividad Química, Centro Atómico Constituyentes, Comisión Nacional de Energía Atómica, Avenida del Libertador 8250, 1429 Buenos Aires, Argentina

Received 8 October 1998; accepted 7 December 1998

Contents

Abstract

Upon exposure to liquid water or to aqueous solutions, the surfaces of metal oxide particles or films undergo a series of chemical reactions that are dictated to a large extent by the chemistry of the metal ions involved. These reactions involve surface hydroxylation and hydration (dissociative and non-dissociative water chemisorption), chemisorption of solutes and charge transfer reactions. The present review focuses on the chemisorption of anions, which is a surface complexation reaction. In simple cases, chemical equilibria may be written, and quantified by heterogeneous stability constants that resemble the analogous homogeneous ones. This approach has been practiced for more than 20 years, and in selected cases values are available for a discussion of stability trends, even though the stability constant

* Corresponding author. Tel.: +54-11-4704-1411; fax: +54-11-4704-1164.
E-mail address: miblesa@cnea.gov.ar (M.A. Blesa)

PII: S0010-8545(99)00005-3

values are sensitive to double-layer modeling and to the history of the metal oxide used. Most of the stability constants have been derived in conventional ways from measurements of the corresponding adsorption isotherms, a procedure that does not provide structural information. Modeling of the shape and pH dependence of adsorption isotherms has been however used to propose various modes of adsorption, in order to derive, for instance, the speciation of surface complexes as a function of ligand concentration and pH. Presently, structural techniques are available to probe directly into the structure of the surface ensembles; the use of UV–vis, IR, magnetic and surface spectroscopies, together with EXAFS and SEXAFS has provided credence to the surface complexation approach, as discussed in the present review for selected cases. In particular, attenuated total refection FTIR has proved to be a powerful tool to derive the surface speciation in selected cases. The reactivity patterns of the surface complexes is being currently explored. The catalysis of ester hydrolysis, the rates and mechanisms of oxide dissolution, heterogeneous charge transfer reactions and the photocatalytic reactions of oxidation of organic compounds can all, in certain cases, be described as reactions of specific surface complexes; some relevant examples are discussed.

Keywords: Chemisorption; Surface complexes; Metal oxides; Oxide dissolution; Heterogeneous catalysis

1. Introduction

The impressive wealth of information available on the chemistry of dissolved metal ions contrasts with the 'low resolution' knowledge about the chemistry of the metal oxide/water interface. It was realized long ago that close similarities exist between both chemistries. For instance, as early as 1954, Myers and Taube [1] demonstrated that the dissolution of $CrCl_3(s)$ was catalyzed by $Cr^{2+}(aq)$. The catalysis involving electron transfer is a widespread phenomenon (as discussed below), closely related to homogeneous electron transfer between metallic centers.

The spectroscopic tools now available have provided evidence in favor of the ideas first put forward in the 1960s, describing the chemisorption of anions onto metal oxides as a surface complexation equilibrium characterized by a surface complexation constant [2–5]. Earlier, Parks and de Bruyn [6] had described the acidity of metal oxide particles as a result of protolytic reactions involving the surface metal ions; the amphoteric nature of the oxide particles derives from two successive equilibria. The standard description of the chemical phenomena involved in protolytic and anion adsorption equilibria is given by Eqs. (1)–(3):

$$\equiv M-OH_2^+ \rightleftarrows \equiv M-OH + H^+ \quad (1)$$

$$\equiv M-OH \rightleftarrows \equiv M-O^- + H^+ \quad (2)$$

$$\equiv M-OH + HX^- \rightleftarrows \equiv M-X^- + H_2O \quad (3)$$

Several conventions have been used in these equations:

1. The symbol ≡ represents the set of bonds linking the surface ion M to the solid framework; usually, the exact coordinative arrangement around M is not

known, and a wide variety of suggestions about this feature have been put forward. The simplest one is the assumption that chemisorption of water provides the required number of ligands to achieve full coordination around M. There is a wealth of information about water chemisorption, both dissociative and molecular; this subject is discussed in Section 2. The details of the coordinative arrangement have been postulated to determine the acidity of the surface groups, in a fashion that is described in more detail below.

2. The two acidity equilibria (Eqs. (1) and (2)) may involve either two protolytic reactions of water molecules bound to the same surface M ion, or reactions on two different sites, the acidic group being either $-OH_2^{n+}$ or $\equiv OH^{m+}$. The single dash in the former case indicates water bound to a single metal ion, whereas, as before, $\equiv O^{(1-m)-}$ are multiple bound oxide groups. These two approaches are discussed below.
3. Anion adsorption has been written as a ligand exchange reaction. The choice of HX^- serves to stress that strong chemisorption is more often than not associated with multiple charged anions stemming from weak Brønstead acids. Furthermore, the higher affinities pertain to chelating anions, such as oxalate, that might form a mononuclear chelate ring, or a more extended bridge involving two surface ions. Adsorption may, as indicated in Eq. (3), change the surface charge density, or it may not; several alternate possibilities for the surface complexation by oxalate are shown in Fig. 1.

The development of the surface complexation approach has lead to a body of stability constants. The involved surface complexes are characterized by their degree of protolysis and by the number of surface ions and ligands involved in the formation of the complex; surface speciation is of course much more speculative and tentative than solution speciation.

This review is arranged as follows. In Section 2, experimental evidence and theoretical calculations on the chemisorption of water shall be presented. In Section 3, the formal approaches to describe the chemisorption of anions shall be discussed. Two different aspects are involved: the description of the intrinsic ('chemical') affinity of surface ions for complexing agents, and the perturbations brought about by the development of charge in the interface. Our focus shall be in the first point, although all of the experimental evidence is strongly influenced by the second aspect. In particular, the derivation of surface acidity constants, or surface complex stability constants, from adsorption data requires that a given model of the electrical double layer be assumed, and that the locus of the adsorbing ions be defined. Fig. 2 shows the charge–potential relationships according to some of the most widely used models of the double-layer region: the Gouy-Chapman diffuse double layer, the constant capacitance double layer, and the triple layer that combines features of the previous two. Table 1 summarizes the charge–potential relationships that describe these models.

The surface complexation approach, as it stands presently, shows all the virtues and limitations of its very simple, swamping assumptions. In Section 4, spectroscopic and related evidence shall be reviewed; certainly, it is expected that in the near future these tools will lead to a more precise description of the nature of the

interactions. In Section 5, the reactivity of surface complexes will be reviewed: kinetics of substitution, acid attack on pendant oxo groups (ligand assisted dissolution), heterogeneous charge transfer, and catalysis of ligand transformation.

2. The chemisorption of water onto metal oxides

The first stage of surface hydration involves the formation of surface hydroxide groups (dissociative adsorption); theoretical calculations for TiO_2 surfaces [7] demonstrate that symmetrical, molecularly adsorbed water is unstable, and that the activation barrier for evolution to a fully dissociated configuration is low. Synchrotron radiation photoemission demonstrates both forms of adsorption on (100) faces [8]. High resolution electron energy loss spectroscopy demonstrates that adsorption on (110) faces originates three different layers as water vapor pressure increases; the first layer is composed of dissociated molecules ($\nu(OH) = 3690\ cm^{-1}$), whereas the second layer is due to molecular adsorption ($\nu(OH) = 3420–3505\ cm^{-1}$;

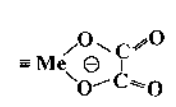

I

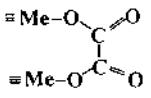

II

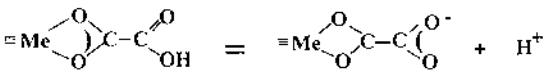

IIIa IIIb

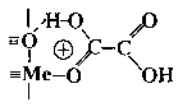

IV

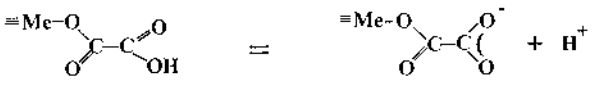

Va Vb

Fig. 1. Some possible oxalato–surface complexes. Species linked by protolytic equilibria are indicated as a and b.

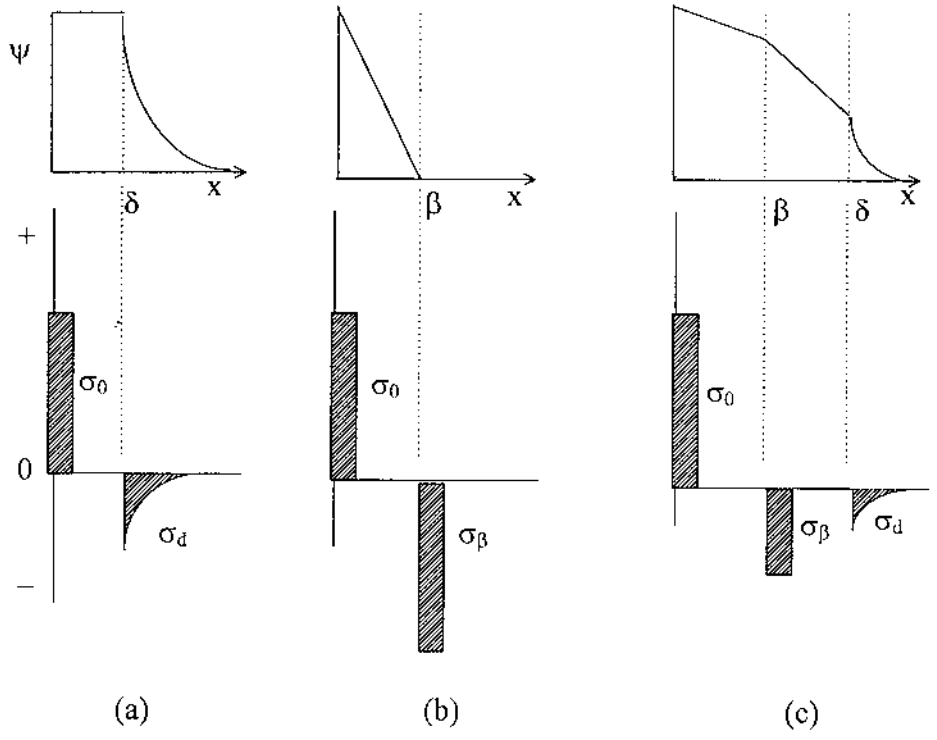

Fig. 2. Sketch representation of the most commonly used models of the electrical double layer. The upper part depicts how the electrostatic potential varies with the distance from the oxide surface. The lower part indicates the corresponding distributions of charge. (a) Gouy-Chapman diffuse double layer; (b) constant-capacitance double layer; (c) triple layer.

$\delta(\mathrm{HOH}) = 1625\ \mathrm{cm}^{-1}$). Hydrogen bonding between molecular water and OH groups is also indicated by a red shift of the O–H stretching frequency [9]. Water adsorption on (100) surfaces has been quantified using the O 1s X-ray photopeak from OH groups; for nearly defect-free surfaces, water coverage of one quarter of

Table 1
Charge–potential relationships corresponding to models of the double-layer region (see also Fig. 2): (a) Gouy-Chapman diffuse double layer; (b) constant-capacitance double layer; (c) triple layer

	a	b	c
Electroneutrality	$\sigma_0+\sigma_d=0$	$\sigma_0+\sigma_\beta=0$	$\sigma_0+\sigma_\beta+\sigma_d=0$
Charge-potential relationships	$\sigma_d{}^a = -11.74c^{1/2}\sin h\left(-\frac{e\psi}{2kT}\right)$	$\psi_0=\sigma_0/C^b$	$\sigma_d{}^a = -11.74c^{1/2}\sin h\left(-\frac{e\psi}{2kT}\right)$; $\psi_0-\psi_\beta=\sigma_0/C_1$; $\psi_\beta-\psi_d=\sigma_\beta/C_2$

[a] For aqueous solutions at 25°C.
[b] C, (constant) capacity; subscripts 1 and 2 refer to the inner and outer constant capacity layers of the triple layer model.

a monolayer is achieved upon liquid water exposure. In defective surfaces, defects created by electron beams were completely removed by liquid water [10].

In other cases, the hydroxylation reaction is strongly limited by high activation energies. For example, in the case of silica, totally dehydroxylated surfaces are highly hydrophobic, and hydroxylation may be achieved only under strong conditions (high temperature and/or aggressive chemicals) [11,12].

Hydroxylation may be viewed therefore as the first surface complexation reaction in aqueous media, since it originates surface hydroxocomplexes. In principle, dissociative chemisorption of water generates at least two different surface complexes that differ in the coordination number of oxygen in –OH groups; the following scheme shows the process:

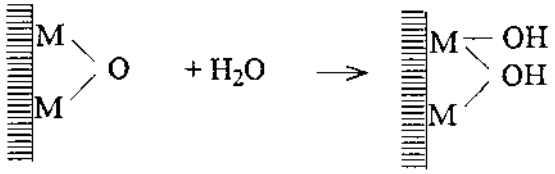

(4)

Such a simple process is however often complicated because of two factors:

(i) Ensuing reactions may occur that restore the coordination environment around M, as in the case of silica:

(5)

(ii) In the surface of oxides, more than one type of metal ions may be present, and consequently several surface hydroxide groups may form. For example, in goethite, α-FeOOH, four different ≡Fe–OH groups may be identified; in two of them, the coordination number of oxygen is 1, whereas coordination numbers of 2 and 3 characterize the remaining two [13]. As a simple case, we can mention the (001) surface of anatase (TiO_2). Dissociative water chemisorption can be depicted as in Eq. 4, [14]. Thus, $\equiv M\text{–}OH^{(1/3)-}$ and $\equiv OH^{(1/3)+}$ surface sites are generated; the indicated charges are calculated according to Pauling rules. These two sites, usually designated as A and B, account for the basic (A sites) and for the acid properties (B sites) of flat surfaces. On real surfaces, further, lower coordination number ions must also be taken into account (ions at kinks, edges) [15].

These crystallographic considerations have been pursued in considerable detail in some models of the surface complexation of metal ions [16–19]. Needless to say, this conceptually correct description often collides with the dearth of experimental information.

Following the original hydroxylation, and depending on the degree of coordinative unsaturation, further water chemisorption takes place, yielding ensembles of the type $\equiv M(OH)_n(H_2O)_m$, where n is determined by charge balance considerations, and $(n+m)$ is determined by coordination requirements; these ensembles are also representative of hydrous metal oxides, i.e. hydrated, amorphous metal oxides. The

species, as written, represents an uncharged moiety; it may undergo protolytic reactions that place negative or positive charges on the surface. Eqs. (1) and (2) are the standard shorthand notation to describe these protolytic reactions in the so-called one-site/two-constants model [5]. This notation should not be interpreted literally; only for highly covalent oxides such as silica, are surface hydroxide groups of the type ≡M–OH acidic enough to undergo deprotonation. In the more general case of oxides of lower-valent cations, ≡M–O$^-$ groups are incompatible with aqueous media, and the source of protons are either surface water molecules [20] or surface hydroxide groups of the type ≡OH. These latter are included in the multiple site MUSIC models [16–19], whereas Lyklema [21], on the basis of the measurement of the temperature dependence of the point of zero charge, postulates that the source of ionizable protons is always chemisorbed water (see also Ref. [20]); if this is the case, Eqs. (1) and (2) should in fact be written as:

$$\equiv M(OH)_{n-1}(H_2O)_{m+1}^{+} \rightleftarrows \equiv M(OH)_n(H_2O)_m + H^+ \quad (6)$$

$$\equiv M(OH)_n(H_2O)_m \rightleftarrows \equiv M(OH)_{n+1}(H_2O)_{m-1}^{-} + H^+ \quad (7)$$

For convenience, we shall use the notation of Eqs. (1) and (2) in what follows, keeping in mind that they are meant to be a shorthand representation of Eqs. (6) and (7).

The values of the constants K_{a1}^{int} and K_{a2}^{int} for the equilibria in Eqs. (1) and (2) determine pH_0, i.e. the pH at which the surface charge σ_0 (and the surface potential ψ_0) at the adsorption plane of protons is zero:

$$pH_0 = \tfrac{1}{2}(pK_{a1}^{int} + pK_{a2}^{int}) \quad (8)$$

When $pH = pH_0$, it is usually true that:

$$N_s \cong \{\equiv M-OH\} \gg \{\equiv M-OH_2^+\} = \{\equiv M-O^-\} \quad (9)$$

The formal similarity between the protolytic equilibria (Eqs. (6) and (7)) and ionic hydrolysis equilibria in homogeneous solutions is obvious; see for instance Eqs. (10) and (11):

$$Fe(OH)_2^+ + H_2O \rightleftarrows Fe(OH)_3(aq) + H^+ \quad (10)$$

$$Fe(OH)_3(aq) + H_2O \rightleftarrows Fe(OH)_4^- + H^+ \quad (11)$$

This similarity lead naturally to attempts to correlate the values of pH_0 with the solution isoelectric point (pH_{siep}), i.e. the pH value at which $[Fe(OH)_2^+] = [Fe(OH)_4^-]$ (assuming that more highly charged species are negligible)[1]. The actual values of pH_0 and pH_{siep} are in fact expected to differ mainly for two reasons:

1. The contribution of solvation to the stability of positive and negative complexes differs for dissolved and surface species. Hydration of cations is expected to be more stabilized in solution, and therefore dissolved cations are less acidic than surface cations. The effect is less important for anions [22–24].

[1] pH_0 describes the condition of zero protonic charge and zero surface potential in the absence of specific adsorption of other ions. When other ions are present (e.g. at the β-plane), the zero protonic charge condition and the condition of zero surface potential diverge in opposite directions from pH_0.

Table 2
Selected (hydr)oxide pH_0 and metal ion pH_{siep} values at 25.0°C

Oxide	pH_0 [Ref.]	pH_{siep}[a]
ZrO_2	6.5 [25]	5.4
Al_2O_3	8.3–9.1 [26,27]	6.7
γ-$Al(OH)_3$	6.7 [28]	6.7
$Cr(OH)_3$	8.3 [23]	8.8
Cr_2O_3	7.9 [23]	8.8
α-Fe_2O_3	8.5 [29]	8.0
α-FeOOH	8.4 [23]	8.0
$Co(OH)_2$	8.3–11.5 [30]	10.9
NiO	9.8–11.5 [30]	10.0

[a] Calculated with data extracted from Ref. [31].

2. The Brønstead acidity of coordinated water is not expected to be equal for $M(OH)^+_{n-1}(aq)$ and $\equiv M-OH_2^+$, or for $M(OH)_n(aq)$ and $\equiv M-OH$. The diverse character of the coordination shell around M leads to differing acidities. From a fundamental point of view, the acidity of surface complexes could be estimated a priori if the structural characterization of the complex were available. This approach is carried out by Hiemstra et al. [16–19].

The solvation effect can in principle be dealt with in a general way; the structural aspects on the other hand are specific and, even though more precise, may lead to the need to specify a vast variety of surface sites that depend on the sample history (exposed faces, defects structure, degree of surface reconstruction, etc.).

The qualitative parallels between pH_0 and the pH_{siep} are illustrated in Table 2 [5,23,24].

Eq. (1) does not lead to a simple Langmuirian dependence of $\{\equiv M-OH_2^+\}$ on $[H^+]$ because K_{a1} is sensitive to the local potential. The potential profiles shown in Fig. 2 change with the degree of coverage, and the solution of Eq. (1) requires that a series of coupled equations also be considered; these are the equations shown in Table 1, and the standard equation describing the dependence of K_{a1} on local potential. A simple, and much used explicit relation results when the constant-capacitance model applies (Fig. 2b):

$$[H^+] = K_{a1}^{int} \frac{\{\equiv M-OH_2^+\}}{N_s - \{\equiv M-OH_2^+\}} e^{\frac{F^2\{\equiv M-OH_2^+\}}{CRT}} \quad (12)$$

In Eq. (12), $F = 96\,500$C and C is the capacitance.

3. Chemisorption of anions

The surface complexation approach describes the chemisorption of anions onto metal oxides as a substitution process whereby the incoming anion substitutes for water molecules (or their protolysis products) in the first coordination sphere of

surface metal ions. In the triple-layer model, adsorption may also take place in the form of outer-sphere ion pair formation. It is obvious that this combination of possibilities suggests a chemisorption mechanism that is equivalent to the well known Eigen–Wilkens mechanism for substitution in dissolved metal ions. Section 5.1 deals with the kinetics of substitution, but it is adequate to describe the heterogeneous 'Eigen–Wilkens' mechanism now:

$$\equiv M\text{–}OH_2^+ + X^{n-} \rightleftarrows \equiv M - OH_2^+ \cdots X^{n-};\ K_{os} = \frac{k_{os}^f}{k_{os}^r} \tag{13}$$

$$\equiv M\text{–}OH_2^+ \cdots X^{n-} \rightarrow \equiv M\text{–}X^{n-1} + H_2O;\ k_{ex} \tag{14}$$

The initial rate R_0 (for very low degrees of coverage, $\theta \rightarrow 0$), is therefore given by:

$$R_0 = \frac{N_s k_{ex} k_{os}^f [X^{n-}]}{k_{os}^f [X^{n-}] + k_{os}^r + k_{ex}} \tag{15}$$

Several simple limiting cases arise for R_0:

(i) High stability of the ion pairs (large K_{os}), and low rate of water exchange (small k_{ex}):

$$R_0 = N_s k_{ex} \tag{16}$$

(ii) Low steady-state concentration of ion pairs, due to small K_{os}:

$$R_0 = N_s k_{ex} K_{os} [X^{n-}] \tag{17}$$

(iii) Low steady-state concentration of ion pairs, due to large k_{ex}:

$$R_0 = N_s k_{os}^f [X^{n-}] \tag{18}$$

When the inner surface complexation reaction (Eq. (14)) approaches equilibrium as shown in Eq. (19), the surface concentration of the inner sphere complex is given by Eq. (20):

$$\equiv M\text{–}OH_2^+ \cdots X^{n-} \rightleftarrows \equiv M\text{–}X^{(n-1)-} + H_2O;\ K_{is} = \frac{k_{ex}}{k_w} \tag{19}$$

$$\{\equiv M\text{–}X^{n-1}\} = \frac{N_s K_{os} K_{is} [X^{n-}]}{1 + (1 + K_{is}^{-1}) K_{os} K_{is} [X^{n-}]} \tag{20}$$

If the relaxation time τ_1 for the outer-sphere equilibrium (Eq. (13)) is less than $0.1\tau_2$ (the relaxation time for the equilibrium in Eq. (19)), the two relaxation times are:

$$\tau_1^{-1} = k_{os}^f [\{\equiv M\text{–}OH_2^+\} + [X^{n-}]] + k_{os}^r \tag{21}$$

$$\tau_2^{-1} = k_w + \frac{k_{ex} K_{os} [\{\equiv M\text{–}OH_2^+\} + [X^{n-}]]}{1 + K_{os} [\{\equiv M\text{–}OH_2^+\} + [X^{n-}]]} \tag{22}$$

A relaxation behavior of this type was observed by Grossl et al. in a pressure-jump study of the adsorption of chromate and arsenate onto goethite [32]. Their conclusion is however that the first step is the formation of an inner-sphere

complex, that more slowly evolves into another surface complex. The main conclusion remains that the formation of the final, stable surface species probably involves, in the general case, a sequence of transformations, the first one being the transfer of the ligand from solution to the surface, and the latter ones corresponding to surface reactions. A recent paper on the adsorption of sulfate onto hematite [33] suggests that the picture of adsorbed species being either inner- or outer-sphere complexes might be over simplistic, each species detected being in fact a group of different species linked kinetically in such a way that the weighted population average defines the observed properties.

In general, there is very little information about rates of substitution; in most cases the rates are assumed to be 'fast', in the sense of the reaction being complete in a few minutes. The most important features of interfacial kinetics are discussed in Section 5; the remainder of this section will be devoted to a discussion of surface complexation equilibria. (For a critical review of this subject, see Ref. [34]).

Outer-sphere complexation (Eq. (13)) is assumed to be governed by electrostatic factors, that determine their main features. The locus of adsorption is the Stern, or inner Helmholtz, plane of the electrical double layer, characterized by a macropotential ψ_β (see Fig. 2); the Gibbs energy of adsorption associated with the macropotential is:

$$\Delta G_{os} = -ze\psi_\beta \tag{23}$$

In addition, a specific contribution is assumed to describe the local interaction between the sites, with a specific interaction potential ϕ_β that adds to ψ_β. The net result is an intrinsic affinity constant, often assumed to be of the order of 100 dm^3 mol^{-1}. Further to the value of z, the distance from the surface (determined, inter alia, by the size of the anion and the capacitance of the inner region of the double layer), also influences the affinity. The value quoted above, 100 dm^3 mol^{-1}, results from modeling and/or fitting of experimental data; it is model-sensitive, and its usage is restricted to triple-layer pictures of ionic adsorption.

Adsorption Gibbs energies result in fact from an electrostatic contribution, a solvation term, and an intrinsic ('chemical') energy [35]. The electrostatic contribution differs from the ion-pairing energy in solution in the sense that the macropotential ψ replaces the point-charge interactions. The solvation energy, as discussed above, may alter the trends of stability found in homogeneous solution, depending on the hydrophilic/hydrophobic nature of the ligand. Huang et al. [36] have recently estimated the relative contribution of the three factors to the adsorption of chromate onto titanium dioxide: depending on pH and the degree of coverage, they derive the values $\Delta G_{solv} = 0.003$–0.013, $\Delta G_{coul} = (-0.8) - (-1.7)$, $\Delta G_{chem} = (-3) - (-11)$ kJ mol^{-1}, giving credence to the description of chemisorption as a surface complexation reaction. Of course, the picture may differ appreciably for other ligands, especially large, neutral organic molecules; the question is particularly important for the interaction of photosensitizer dyes with titanium dioxide, such as ruthenium–bipyridyl derivatives. Duffy et al. [37] report that FTIR data (see below) strongly suggest surface coordination by carboxylate groups in the frequently used 2,2′-bipy-4,4′-dicarboxylate and its Ru(II) complexes.

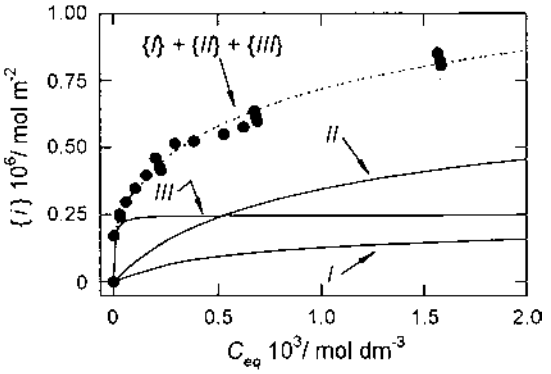

Fig. 3. Speciation of surface Ti(IV)–salicylate complexes as a function of salicylic acid concentration at pH 3.6; $T = 298$ K; note that the sum $\{I\} + \{II\} + \{III\}$ equals the surface excess Γ; symbols are experimental Γ values. The structures of the complexes are shown in Table 3. From Ref. [15].

The Gibbs adsorption energy for inner-sphere complexation may be derived from the measured adsorption isotherms. Analysis of the experimental data usually leads to the conclusion that more than one surface complex may form, depending on the experimental conditions. The most important variables are ligand concentration and pH, and the surface site density is usually treated as an adjustable parameter that may differ for the various types of surface complexes. Thus, a set of adsorption isotherms measured at different pH values is transformed into a set of surface complexation stability constants, and surface speciation diagrams may be derived. As an example, Figs. 3 and 4 show adsorption isotherms of salicylic acid onto titanium dioxide, together with the derived surface speciation diagrams [15]. The

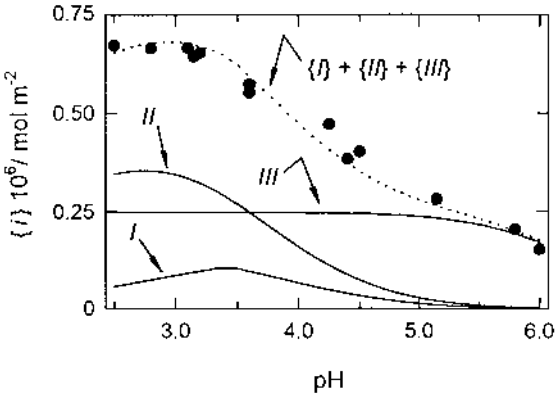

Fig. 4. Speciation of surface Ti(IV)–salicylate complexes as a function of pH at 298 K; note that the sum $\{I\} + \{II\} + \{III\}$ equals Γ; symbols are experimental Γ values. The structures of the complexes are shown in Table 3. Other conditions are: total salicylic acid concentration: 8.0×10^{-4} mol dm^{-3}; surface-to-volume ratio: 514 m^2 dm^{-3}. From Ref. [15].

Table 3
Surface complexation equilibria and their corresponding constants for adsorption of salicylate onto titanium oxide (cf. Figs. 3 and 4)[a]

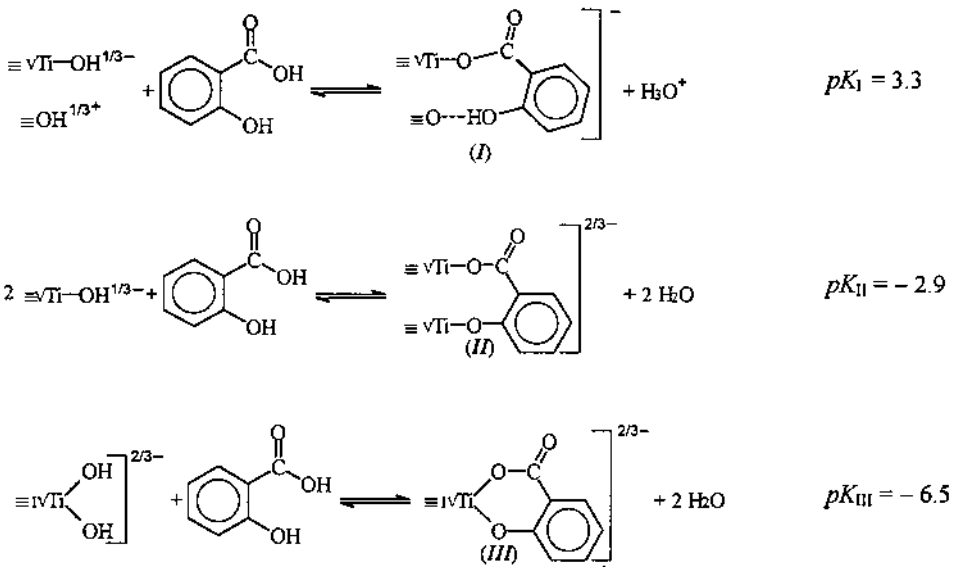

[a] The small roman numeral preceding Ti indicates number of oxobonds.

surface complexation equilibria and their corresponding constants are shown in Table 3.

The modeling of adsorption of carboxylates is usually rather involved, because the more strongly chemisorbing anions are polyprotic and multidentate, and the variety of surface complexes that may result is very large. In Section 4 we shall discuss the spectroscopic evidence; now we shall use the results of Nowack and Sigg [38] on the adsorption of EDTA on goethite, as an example of the information that can be derived from adsorption isotherms. Previous work by Matijevič and co-workers may also be consulted [39–41]. Nowack and Sigg measured the amount of adsorbed EDTA as a function of EDTA concentration at various pH values and the results were complemented with the measurement of the stoichiometry of the desorption reaction produced by addition of phosphate. From the experimental data, it was possible to derive information about the parameters n and m in Eq. (24), where $H_4Y = EDTA$:

$$n{\equiv}Fe{-}OH + Y^{4-} + (m+n)H^{+} = {\equiv}Fe_nLH_m^{(4-n-m)-} + nH_2O \quad (24)$$

Both the number of surface metal ions complexed by one EDTA ligand and the degree of protonation of the surface complex could thus be derived. Our earlier

work [42] shows that in fact two consecutive surface complexation stages were suggested by the shape of the adsorption isotherm onto magnetite. Nowack and Sigg find that two different surface complexes are required to account for the data, corresponding to ($n=2$, $m=1$) and ($n=1$, $m=0$). The two equations are:

$$2{\equiv}Fe{-}OH + Y^{4-} + 3H^{+} = {\equiv}Fe_2YH^{-} + 2H_2O;\ \log K = 30.36 \quad (25)$$

$${\equiv}Fe{-}OH + Y^{4-} + H^{+} = {\equiv}FeY^{3-} + H_2O;\ \log K = 14.99 \quad (26)$$

The stability constants were derived using a generalized two-layer model for the interfacial region [43] (see Fig. 2).

These two modes of adsorption represent in fact the successive formation of two complexes, the second step being:

$${\equiv}Fe_2YH^{-} + Y^{4-} = 2{\equiv}FeY^{3-} + H^{+};\ \log K = -0.38 \quad (27)$$

$\equiv FeY^{3-}$ contributes appreciably to the surface speciation only at high pH values, as expected from Eq. (27). The degree of protonation of $\equiv Fe_2YH^{-}$ suggests that at least one of the carboxylate groups is not bound to Fe; the reverse inference, that no free groups are present in $\equiv FeY^{3-}$, cannot be taken because deprotonation may simply be due to electrostatic effects. Note that the predominant species of free EDTA in the spanned pH range is H_2Y^{2-}; further deprotonation upon complexation is to be expected.

It is clear that good coordinative groups for ions in solution are also good complexing agents for the same ions in the surface of the oxide. Thus, carboxylates and phenolates, especially when chelating, form strong surface complexes with titanium dioxide and with Ti(IV) in solution [44,45]. Vasudevan and Stone [46,47] measured the adsorption isotherms of 4-nitrocatechol, 4-nitro-2-aminophenol and 4-nitrophenylendiamine onto TiO_2, Fe_2O_3, FeOOH and Al_2O_3. They found that in all cases the general trend of stability was catechol > 2-aminophenol $\gg$ *o*-phenylendiamine, and that the trend for catechol was TiO_2 > Fe(III) (hydr)oxides > Al_2O_3. For different TiO_2 samples, significant differences in stability were found, indicating that the detailed surface topology was an important factor. It is likely that, following the pioneer work of Stone (see Ref. [48]), the systematic study of stability trends, common in solution chemistry (Irving-Williams, nephelauxetic series), will provide in the future a good insight in the nature of surface complexation.

In the case of complexation of hydrous ferric oxide by simple inorganic anions, a critically assessed set of stability constants has also been derived from adsorption isotherms using a generalized two-layer model for the interfacial region [43]. Table 4 shows selected values of surface complexation constants and of acidity constants of the surface complexes, corresponding to the following equations:

$${\equiv}Fe{-}OH + XO_4^{2-} + H^{+} \rightleftarrows {\equiv}Fe{-}O_4X^{-} + H_2O;\ K_1 \quad (28)$$

$$\equiv Fe\begin{matrix}O_4X^{-}\\ OH_2^{+}\end{matrix} \rightleftharpoons \equiv Fe\begin{matrix}O_4X^{-}\\ OH\end{matrix} + H^{+};\ K_{a1} \quad (29)$$

Table 4
Complexation and acidity constants of surface complexes formed by inorganic anions (cf. Eqs. 28 and 29)

Anion	pK_1	pK_{a1}
SO_4^{2-}	7.8	7.0
SeO_4^{2-}	7.7	6.9
SeO_3^{2-}	12.7	7.5
CrO_4^{2-}	10.8	–

In fact, the experimental adsorption data provide information about the stoichiometric ratio of ligands and protons in the surface complex, but do not identify the basic sites for proton binding. Of course, an obvious possibility is the pendant oxygen atoms of the oxoanions; the high pK_a values (close to 7) for the sulfate(VI), selenate(VI) and selenate(IV) surface complexes suggest however, that protons may rather be exchanged by proximal water molecules. In agreement, there is no correlation between the surface pK_a values and the acidities of HSO_4^- and $HSeO_4^-$. In the case of phosphate(V) and arsenate(V), the pK_a values of the surface complexes are not very different from the pK_a of $H_2XO_4^-$, and both possibilities remain valid. Some attempts have been made to correlate the stability of surface and aqueous complexes; Fig. 5, redrawn from Ref. [43], shows a tentative LGER plot for the case of divalent oxoanions.

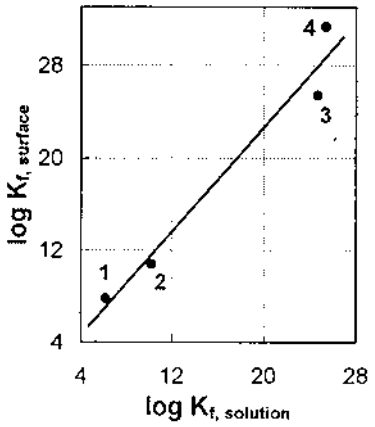

Fig. 5. Comparison of surface and homogeneous stability constants for complexes of simple inorganic anions with Fe(III). The anions considered are: **1**: $SO_4^=$; **2**: $CrO_4^=$; **3**: $HPO_4^=$; **4**: $H_2PO_4^-$. Redrawn from Ref. [43].

4. Spectroscopic and structural characterization of surface complexes

A wide variety of techniques have been used to probe the structure of surface complexes; for a detailed treatment, see Ref. [49]. However, most of the methods are especially suited to study heavy elements, and thus have been mostly used to study cationic adsorption; perhaps the best characterized anions are the oxoanions of heavy elements, like arsenate(V) or selenate(VI) (see below).

Since the pioneer work of Tejedor-Tejedor and Anderson [50], FTIR and visible diffuse reflectance have yielded the most valuable information about the chemisorption of organic anions up until now. This situation is to be contrasted with the detailed exploration of surfaces under high vacuum conditions, that can be provided by the synchrotron techniques, as well as by the many variants of electron spectroscopies and electron diffraction methods (HREEL, LEED).

When the spectrum of surface species at the solid/water interface is sought, a most serious problem is that the signal from the adjoining solution volume is in general orders of magnitude larger than that due to surface species, and the shifts are usually small enough to prevent resolution. The advent of the attenuated total reflection FTIR (ATR-FTIR) method has largely solved this problem, because the thickness probed by the evanescent radiation is of the order of 1 μm for 45° incidence angle. UV–vis diffuse reflectance data also have served as a characterization tool; in this case, spectra are usually obtained on dry rinsed samples, in which expected loose ligands have been removed.

Table 5 summarizes published ATR-FTIR studies of the adsorption of anions onto metal oxide surfaces. The table also includes studies based on ex-situ IR and Raman techniques, such as diffuse reflectance FTIR and FT-Raman.

The chemisorption of simple carboxylates has been studied in some detail. Oxalate adsorption onto TiO_2 [69] and onto hydrous chromium oxides [70] have been demonstrated by the ATR-FTIR spectroscopy. Data collected on titanium dioxide as a function of ligand concentration and pH could be interpreted as being due to the formation of three different surface complexes, the spectra of which could be derived by factor analysis of the spectra collected at different pH values. The mathematical procedure requires that a chemical model of the interaction be assumed; Hug and Sulzberger assumed that the three different complexes are formed independently.

In the case of salicylate adsorption onto TiO_2 [71] two adsorption modes are identified. Two different chemical models, corresponding to the formation of two different independent complexes and to two successive complexation steps, were analyzed:

(i) Independent adsorption:

$$x{\equiv}S + C_6H_4(OH)COO^- + nH^+ \rightleftarrows {\equiv}S_x(C_6H_4(OH)COO)H_n^{(n-1)+} \quad (30)$$

$$y{\equiv}S + C_6H_4(OH)COO^- + mH^+ \rightleftarrows {\equiv}S_y(C_6H_4(OH)COO)H_m^{(m-1)+} \quad (31)$$

(ii) Successive adsorption:

$$x{\equiv}S = C_6H_4(OH)COO^- + nH^+ \rightleftarrows {\equiv}S_x(C_6H_4(OH)COO)H_n^{(n-1)+} \quad (32)$$

Table 5
Summary of IR and Raman studies of surface complexes formed by adsorption of ligands at the metal oxide/aqueous solution interface

Ligand	Oxide	Technique	Ref.
Sulfate(VI)	Hematite (α-Fe_2O_3)	ATR-FTIR	[33,51]
		Transmission IR	[52]
	Goethite (α-FeOOH)	Diffuse reflectance FTIR	[53]
		Transmission IR	[54]
	Fe(III) oxides	Transmission IR	[55]
	Aluminum hydroxide gel	Transmission IR	[56]
Phosphate(V)	Hematite and Goethite	Diffuse reflectance FTIR	[57]
	Goethite	ATR-FTIR	[50]
		Transmission IR	[13,58]
Methylphosphonate	Goethite	ATR-FTIR	[59]
Phenylphosphonate	γ-Al_2O_3 and bohemite (γ-AlOOH)	Diffuse reflectance, ATR-FTIR and FT-Raman	[60]
Halides (F^-, Cl^-, Br^-, I^-)	Goethite	Transmission IR	[61]
Nitrate	Goethite	Transmission IR	[61]
	Aluminum hydroxide gel	Transmission IR	[56]
Carbonate	Goethite	Transmission IR	[62]
		FTIR	[63]
	ZrO_2	ATR-FTIR	[64]
Selenate(III)	Goethite	Transmission IR	[61]
Arsenate(V) and arsenate(III)	Goethite	ATR-FTIR	[65]
	Goethite	Transmission IR	[66]
Oxalate	Goethite	Transmission IR	[67]
	Gibbsite ($Al(OH)_3$)	Transmission IR	[68]
	TiO_2 (anatase)	ATR-FTIR	[69]
	Cr(III) hydrous oxides	ATR-FTIR	[70]
Malonate	TiO_2 (anatase)	ATR-FTIR	[71]
Lactate, tartrate and citrate	Goethite and $Fe(OH)_3$	Transmission IR	[72]
Acetylacetone	TiO_2, ZrO_2 and Al_2O_3	ATR-FTIR	[73]
Benzoate	Goethite	ATR-FTIR	[74]
		Transmission IR	[67]
	Gibbsite ($Al(OH)_3$)	Transmission IR	[68]
	TiO_2 (anatase)	ATR-FTIR	[75]

Table 5 *(Continued)*

Ligand	Oxide	Technique	Ref.
Phthalate	Goethite	ATR-FTIR	[76]
		Diffuse reflectance FTIR	[77]
	Hematite	Diffuse reflectance FTIR	[78]
	TiO_2 (anatase)	ATR-FTIR	[75]
p-Hydroxibenzoate	Goethite	ATR-FTIR	[76]
	Fe(III) oxides	Diffuse reflectance FTIR	[79]
p-Substituted benzoates	Fe(III) oxides	Diffuse reflectance FTIR	[80]
Salicylate	Goethite	ATR-FTIR	[81,82]
	Fe(III) and Al(III) oxides	ATR-FTIR	[83]
	TiO_2 (anatase)	ATR-FTIR	[75]
	Illite clay	ATR-FTIR	[84]
2,4-Dihydroxibenzoate	Goethite	ATR-FTIR	[76]
2-Aminobenzoate	TiO_2 (anatase)	ATR-FTIR	[75]
Phenols	Fe(III) oxides	Diffuse reflectance FTIR	[85]
Chlorophenols	Fe(III) oxides	Diffuse reflectance FTIR	[86]
Catechol	Amorphous alumina and bohemite	Transmission and diffuse reflectance FTIR	[87]
	Hematite	Diffuse reflectance FTIR	[78]
	TiO_2, ZrO_2 and Al_2O_3	ATR-FTIR	[73]
4-Chlorocatechol	TiO_2 (anatase)	ATR-FTIR	[88]
8-Quinolinol	TiO_2, ZrO_2 and Al_2O_3	ATR-FTIR	[73]
Bipyridine	TiO_2 (anatase)	ATR-FTIR	[71]
2,2′-Bipyridine-4,4′-dicarboxylate	TiO_2 (anatase)	ATR-FTIR	[71]
2,2′-Bipyridine-4,4′-dicarboxylate and several of its Ru(II) complexes	TiO_2	ATR-FTIR	[37]
Bis or trisbipyridylruthenium(II) and carboxylated derivatives	TiO_2	Raman	[89]
Phenylfluorone	TiO_2	FTIR	[90]
Hydroxamate	Goethite	ATR-FTIR	[91]
Laurate	Corundum (α-Al_2O_3)	ATR-FTIR	[92]
Oleate	Hematite	Transmission IR	[93]
	Ilmenite ($FeTiO_3$)	Transmission IR	[94]

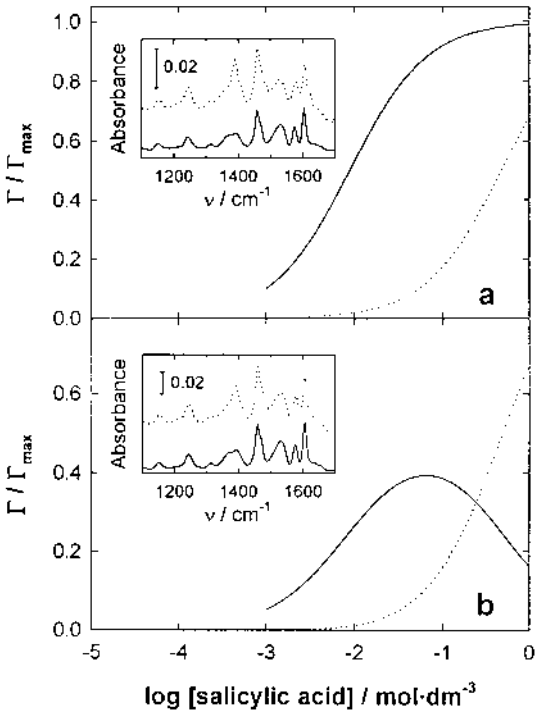

Fig. 6. Calculated adsorption isotherms (in linear-log scale) for the two adsorption modes of salicylate onto TiO_2 (a) two-sites, independent adsorption; (b) one-site, successive adsorption. The best fitting apparent stability constants at pH 4.0 are, respectively, (a) $\log K_{30} = 5.05$, $\log K_{31} = 3.32$; (b) $\log K_{32} = 4.75$, $\log K_{33} = 3.61$. Insets: FTIR spectra of the two surface complexes. Experimental conditions: 298 K, pH 4.0, 0.01 mol dm^{-3} ionic strength. From Ref. [71].

$$\equiv S_x(C_6H_4(OH)COO)H_n^{(n-1)+} + C_6H_4(OH)COO^- \rightleftarrows + mH^+$$
$$\rightleftarrows \equiv S_x(C_6H_4(OH)COO)_2H_{n+m}^{(n+m-2)+} \quad (33)$$

Fig. 6 shows the results of modeling the spectra on the basis of the two schemes. In both cases it is assumed that complexation is described by a simple equilibrium constant, unaffected by surface potentials (Langmuirian model). Models (i) and (ii) turn out to be indistinguishable by the goodness of the fitting. Biber and Stumm [83], on the other hand, found out that the surface binding modes of salicylate onto several oxides and oxohydroxides differ depending on the nature of the metal ion and the chemical composition of the (hydr)oxide.

Singular value decomposition of ATR-FTIR spectra of 4-chlorocatechol adsorbed on TiO_2 [88] demonstrates the existence of a single inner-sphere surface complex of the type $\equiv Ti-OC_6H_3ClO-Ti\equiv$, and a non-specific mode (outer-sphere complex?). On the other hand, Connor et al. [73] postulate that FTIR demonstrates that catechol, 8-quinolinol and acetylacetonate bind as bidentate ligands to metal surface ions in TiO_2, ZrO_2 and Al_2O_3, and that some surface ions may bind more than one ligand.

Band assignments have been done in the case of oxalate adsorption onto hydrous chromium oxides [70]. Fig. 7 shows the FTIR spectra of a hydrous oxide sample before, (a) and after, (b) exposure to a solution containing oxalate (0.1 mol dm^{-3}) at pH 3.6. The spectrum of aqueous oxalate, as well as the differential spectrum of dissolved $Cr(C_2O_4)_3^{3-}$ (0.01 mol dm^{-3}) in excess oxalate (0.1 mol dm^{-3}) at pH 4.9, are also shown in (c) and (d).

The hydrous oxide presents peaks at 1560, 1470 and 1390 cm^{-1}; the first one can be attributed to surface hydroxide groups, and the others to anion contamination (carbonate and/or nitrate) [95,96]. There are striking differences in the FTIR spectra of different oxide samples, that reflect a series of surface defects and contaminations. However, after surface conditioning in the initial stages of the interaction with oxalic acid, spectra similar to that shown in Fig. 7b are obtained. The spectrum of dissolved $Cr(C_2O_4)_3^{3-}$ (Fig. 7d) shows peaks at 1700, 1410, and 1260 cm^{-1}, that coincide with the most intense vibrations in $K_3[Cr(C_2O_4)_3]$ and $K[Cr(C_2O_4)_2(H_2O)_2]$ [97]. Free oxalate ions present peaks at 1570 and 1320 cm^{-1} (Fig. 7c). Comparison of the spectra demonstrates that surface complexes with

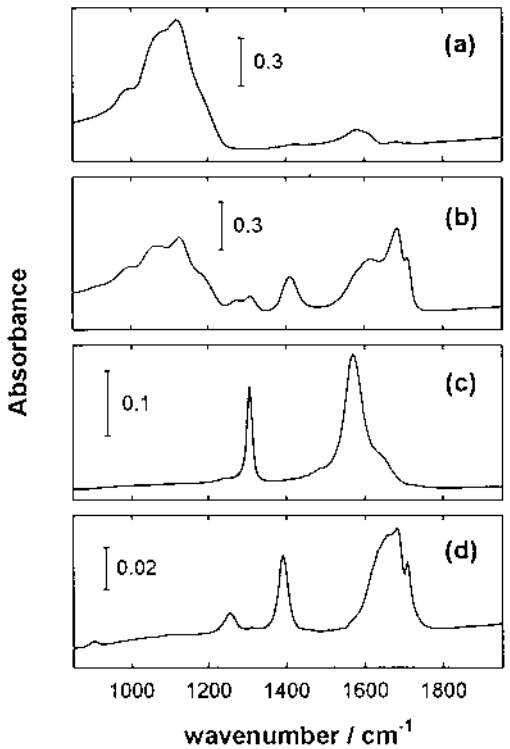

Fig. 7. ATR-FTIR spectra of oxalate adsorbed on chromium(III) oxide. The spectra correspond to a hydrous oxide sample before (a) and after (b) exposure to a 0.1 mol dm^{-3} oxalate solution at pH 3.6. Also shown are the spectrum of aqueous oxalate (c) and a differential spectrum of 0.01 mol dm^{-3} dissolved $Cr(C_2O_4)_3^{3-}$ in 0.1 mol dm^{-3} excess oxalate (d), both at pH 4.9.

chelated oxalate are formed. The main peaks in Fig. 7b (1710, 1680, 1410 and 1260 cm^{-1}) can be attributed to the $\equiv Cr(C_2O_4)$ moiety; the same bands are observed in the solids $K_3[Cr(C_2O_4)_3]$ and $K[Cr(C_2O_4)_2\ (H_2O)_2]$.[69,97]. The shoulder at 1620 and the peak at 1310 cm^{-1} indicate the presence of lesser amounts of uncoordinated oxalate, in agreement with the solution spectrum. No evidence is found of surface $HC_2O_4^-$ species. Although some free oxalate may remain because of incomplete washing of the solution, the peaks assigned to coordinated oxalate can be unambiguously attributed to a surface complex. In this complex, both carboxylate groups are bound, either to the same surface Cr(III) ion or to two adjacent ones. In Fig. 7b some decrease of the bands due to hydroxylated surface sites is also observed, as would be expected if substitution of oxalate for OH takes place.

The combined use of FTIR and scanning tunneling microscopy has proved very valuable to characterize the adsorption of sulfate onto hematite [33]. The splitting of the asymmetric sulfate S–O stretching, located at 1102 cm^{-1}, into three peaks in wet samples and into four peaks in dried samples suggests that inner-sphere complexes are formed, with a possible evolution from monodentate to bidentate upon drying, or from monodentate sulfate to monodentate hydrogenosulfate [51]. STM images, on the other hand, detect highly mobile species with a lifetime in each location in the order of 10–100 ms [33]. From these results, it was concluded that interconversion between different species may in fact be more complicated than generally appreciated.

Spectroscopic studies by means of UV–vis absorption and fluorescence are summarized in Table 6. When applicable, fluorescence emission is especially suited to discriminate between dissolved and surface species. A related phenomenon is the quenching of fluorescence upon adsorption, which provides direct evidence of surface interactions and indirect insight into the nature of the interaction.

EXAFS has been used as a powerful tool to explore the geometry of the species formed upon adsorption. Because of the limitations of the technique, most of the available information refers to the interaction of selected oxoanions with adequate metal oxides. For example, in the case of arsenate adsorption onto goethite, three different Fe–As distances are found, depending on the degree of coverage, at 0.285, 0.324 and 0.360 nm [118]. It is proposed that the species involved are formed by Fe octahedra and As tetrahedra by corner (monodentate) and edge (bridged binuclear and chelated) sharing. Manceau and Charlet [119] on the other hand, find that selenate adsorbs on hydrous ferric ion as bridged binuclear and chelated complexes. Table 7 summarizes the information obtained by EXAFS.

In conclusion, the available experimental evidence validates the idea of surface complexes as quasichemical species that can be described by a stability constant and can be characterized spectroscopically. However, the derivation of stability constants from adsorption data implies the use of a certain model of the double layer and should be used within the frame of the assumptions involved. The spectroscopic characterization is also somewhat limited; it disregards many possible structures, but as a rule it does not provide a unique structural model.

Table 6
UV–vis spectroscopic studies of surface complexes formed by anions adsorbed at the metal oxide/aqueous solution interface

Ligand	Oxide	UV–vis technique	Ref.
Thiocyanate	Hematite (α-Fe_2O_3)	Diffuse reflectance	[98]
	TiO_2	Transmission	[99]
Salicylate	δ-Al_2O_3	Polarized fluorescence	[100]
	TiO_2 (anatase)	Diffuse reflectance	[15,101]
Catechol	TiO_2 (anatase)	Diffuse reflectance	[14,101]
8-Hydroxyquinoline	TiO_2 (anatase)	Transmission	[102]
8-Hydroxyquinoline-5 sulfonate	Al_2O_3	Fluorescence	[103]
Erythrosin B	TiO_2	Transmission and fluorescence	[104]
Eosin	TiO_2	Transmission and fluorescence	[105]
	TiO_2	Internal reflection	[106]
Phenylfluorone	TiO_2	Absorption	[90,107]
Thionine	TiO_2	Transmission and fluorescence	[108]
	TiO_2	Diffuse reflectance	[109]
Pyrene	TiO_2	Absorption and fluorescence	[110]
Phenosafranin	TiO_2, SiO_2	Fluorescence	[111]
9-Anthracene-carboxylate	TiO_2	Transmission	[112]
Rose bengal	TiO_2, Al_2O_3 and SiO_2	Diffuse reflectance and fluorescence	[113]
	TiO_2	Transmission	[114]
Rhodamine B	TiO_2, SiO_2 and ZrO_2	Fluorescence	[115]
Chlorophyll derivatives	TiO_2	Transmission and fluorescence	[116]
1,3,5-Trinitrobenzene	Hectorite clay	Transmission	[117]

5. The reactivity of surface complexes

As stated, the surface complexes exhibit the whole range of chemical reactivity known for dissolved complexes. In this section, we shall first describe some of the peculiar features associated with the substitution mechanisms due to the heterogeneous nature of the process, especially because of the participation of charged interfaces. This description shall be brief because the experimental evidence is very limited, and most of the studies of the complexation reaction itself refer to the time-invariant condition reached after adequate equilibration. On the other hand, there is more information about the changes in reactivity of the pendant oxo groups, brought about by coordination with a different ligand from the solution. In

general, these reactions facilitate dissolution, and the experimental evidence is in the form of rate laws of dissolution. An important part of this section will refer to labilization brought about by electronic effects akin in nature to those well-known in solution (e.g. the *trans* effect), and by internal charge transfer in dimeric surface complexes bridged by a mediating ligand.

5.1. Kinetics of substitution

The Debye-Hückel model of ion solvation and its subsequent modifications lead, in the homogeneous case, to a description of the influence of ionic strength on the rates of ion pair formation and inner-sphere substitution (remember also the work term in the expression of the rates of electron exchange). In the heterogeneous case, the geometry of the interface leads to the Gouy-Chapman model, and the subsequent modifications include the Stern modification. We shall use the triple model of the double layer made popular by Davis and Leckie [35] (see Fig. 2).

The equilibrium constants K_{os} and K_{is} include the effect of electrostatic potential as described by Eqs. (34) and (35):

$$\frac{\{\equiv M\text{–}OH_2^+ \cdots X^{n-}\}}{\{\equiv M\text{–}OH_2^+\}\{X^{n-}\}} = K_{os}^{app} = K_{os} e^{-\frac{ez\psi_\beta}{kT}} \tag{34}$$

$$\frac{\{\equiv M\text{–}X^{(n-1)-}\}}{\{\equiv M\text{–}OH_2^+ \cdots X^{n-}\}} = K_{is}^{app} e^{-\frac{e(\psi_0 - \psi_\beta)}{kT}} \tag{35}$$

This thermodynamic effect manifests itself in different ways in the individual rate constants. The standard electrochemical description yields:

Table 7
Summary of EXAFS studies of surface complexes formed by anion adsorption at the metal oxide/aqueous solution interface

Anion	Oxide	Ref.
Selenate(V)	Goethite (α-FeOOH)	[120]
	δ-$Al(OH)_3$	[121]
Selenate(III)	α-FeOOH	[119,120]
	Hydrous Fe(III) oxides	[119]
Arsenate(V)	Fe(III) oxides	[122]
	Ferrhidryte	[123,124]
	α-FeOOH	[118,124]
	β-FeOOH	[124]
	γ-FeOOH	[124]
Arsenate(III)	α-FeOOH	[125]
Chromate(VI)	α-FeOOH	[118]
	Maghemite (γ-Fe_2O_3)	[126]

$$k_{os}^{f} = k_{os,0}^{f} e^{-\frac{(1-\alpha_{os})ez\psi_{\beta}}{kT}} \quad (36)$$

$$k_{os}^{r} = k_{os,0}^{r} e^{-\frac{\alpha_{os}ez\psi_{\beta}}{kT}} \quad (37)$$

$$k_{ex} = k_{ex,0}^{f} e^{-\frac{(1-\alpha_{is})e(\psi_0-\psi_{\beta})}{kT}} \quad (38)$$

$$k_{w} = k_{w,0}^{f} e^{-\frac{\alpha_{is}ez(\psi_0-\psi_{\beta})}{kT}} \quad (39)$$

where α_{os} and α_{is} are the electrochemical transfer coefficients.

Whereas outer-sphere ion pair formation is most certainly diffusion-controlled, the rates of formation and dissociation k_{ex} and k_{w} of the inner sphere complex require closer inspection. By analogy with solution kinetics, these processes may be associative (A), dissociative (D), or concerted (I_d or I_a); we shall analyze next the behavior α_{is} in each case.

If the process is associative, bond formation with the entering ligand dominates the activation energy; bond rearrangement takes place at the surface plane, and the availability of the entering ligand should be affected by the potential drop ($\psi_0-\psi_{\beta}$). In a dissociative process, on the other hand, the rate is controlled by bond-breaking processes followed by fast transfer of entering and leaving ligands across the potential drop. Thus, in the most simple cases, an influence of the potential profile should be observed if the mechanism is associative (A or I_a), whereas little effect is expected for D or I_d mechanisms.

Actual experimental evidence is scarce. In equilibrated surfaces, the interfacial potentials are determined by the ionic adsorption equilibria themselves. During evolution towards surface complexation equilibrium, the potentials should adjust themselves to the instantaneous charge condition, and in fast reactions they may be affected by the rate of relaxation of the whole double layer to the changing conditions. In other words, the rate of surface complexation determines also ($d\sigma_0/dt$), ($d\psi_0/dt$), and the analogous magnitudes as applied to the β and Stern planes. The rather low typical values for σ_0 suggest, by analogy with solution chemistry, that D or I_d processes are likely.

5.2. Kinetics of dissolution

In mineral, non-complexing acids, the solubility of metal oxides is defined by the solubility equilibrium (Eq. (43)) and by the hydrolytic equilibria of the metal cation.

$$MO_n(s) + 2nH^+ = M^{2n+} + nH_2O \quad (40)$$

The experimental rates of dissolution of several metal oxides in mineral acids have been described in terms of first-order kinetics on adequate surface complexes. In highly undersaturated media, the experimental rate laws are usually of the form given below, with n typically ranging from 0.3 to 2, a very common value being 0.6 [127]:

Table 8
Values of n, the number of adjacent $\equiv M–OH_2^+$ surface complexes that form the critical ensemble that leads to dissolution in acidic media (see also text)

Oxide	n	Ref.
BeO	2	[128]
NiO	2	[129]
Al_2O_3	3	[128]
Fe_3O_4	1	[130]
V_2O_5	1	[131]

$$R = \frac{d[M^{2n+}]}{dt} = k_{exp}[H^+]^n \quad (41)$$

The rate constant k_{exp} depends on the (surface/volume) ratio, on ionic strength, and on the history of the sample. In selected cases, the rate law (Eq. (41)) can be transformed into a first-order law (Eq. (42)), or in a more general expression involving parallel transfer of several surface complexes $\equiv S_i$, Eq. (43):

$$R = k\{\equiv M–OH_2^+\} \quad (42)$$

$$R = \Sigma\, k_i\{\equiv S_i\} \quad (43)$$

For Eqs. 42 or 43 to apply, the protolytic reactions responsible for generating a reactive surface complex must behave as a fast pre-equilibrium. The rate-determining step is associated with the breakage of a critical oxo bond, that is made labile by protonation of the surface moiety (protonation may involve the oxo bond being broken, or adjacent ligands). In some cases, Stumm et al. have postulated an activated state for the dissolution reaction of composition $\{\equiv M^{n+},\ n\equiv H\}^{2+}$ (as opposed to the composition $\{\equiv M^{n+},\ 1\equiv H\}^{2+}$ implied above). Even this more complex composition is traced back to a critical surface ensemble, formed by n adjacent $\equiv M–OH_2^+$ surface complexes. Table 8 summarizes the available information.

In the presence of complexing anions, the rates of dissolution are altered. For our purposes, the most important feature to discuss is the intrinsic reactivity of the surface complexes $\equiv M–L^{n-}$, as measured by the rate of adjacent oxo-bond breaking. There are several reasons why $\equiv M–L^{n-}$ complexes may dissolve faster than $\equiv M–OH_2^+$:

1. The intrinsic reactivity may increase due to inductive effects brought about by changes in the electron density. An enhanced electronic density on the adjacent oxo bonds may favor nucleophilic attack and ensuing dissolution.
2. Adsorption of anions is accompanied by proton coadsorption. The thermodynamic surface excess of protons increases with surface complexation by anions, and therefore the rate of acid dissolution may increase[2]. In acid dissolution, the

[2] Sposito [132,133] has pointed out that an increase in the negative charge density in the β-plane, σ_β (associated with an increase in the adsorption density of anions), is always accompanied by an increase in the positive charge density σ_0 (associated with adsorbed protons).

availability of protons increases the rate. This effect is however, partially compensated for by an increase in positive charge on the metal ion that stabilizes the bond to be broken. Coadsorption avoids this buildup of positive charge. A related consequence is a change in the exponent n in Eq. (41), and therefore, the enhancement brought about may be pH-dependent.

3. A simple thermodynamic factor is the concentration of surface complexes. When the affinity for the ligand L is large, high surface concentrations of $\equiv M-L^{n-}$ may be easily achieved (even saturation coverage is often easily achieved). By contrast, the concentrations of $\equiv M-OH_2^+$ are usually low, except under extremely acidic conditions (in mineral acids, chemisorption of protons is readily arrested by the build-up of positive surface potentials [131].
4. A second thermodynamic factor applies in the case of low solubility, when dissolution is partially balanced by the reverse precipitation process. Complexation in solution enhances (often by orders of magnitude) the solubility of the metal oxide, and the reverse reaction may become negligible.

Casey et al. have carried a systematic study of the dissolution of bunsenite (NiO) in the presence of a variety of ligands, with various functional groups and chelating abilities [129,134–136]. For the series of ligands triethanolamine (tea), glycine (gly), ethylenediamine (en), iminodiacetate (ida) and nitrilotriacetate (nta) they find a good LGER between the measured first-order rate constant k_L of dissolution of surface complexes at pH 8.5 and the stability constant of the complexes in solution (see Fig. 8).

The authors conclude that Ni(II) detaches from the surface as a species closely related to the stable complex in solution, in good agreement with earlier ideas [137,138]. This type of LGER can be established only if precautions are taken to account for the influence of pH on the rate [136].

Dissolution inhibition by surface complexation is also well known; it is usually associated with multidentate complexation, involving several surface metal ions [139].

By far the most dramatic enhancement of the rate of oxo-bond breaking is achieved by changing the oxidation state of the metal ion. The similarity with solution chemistry is straightforward; the lability of oxo bonds is highly sensitive to

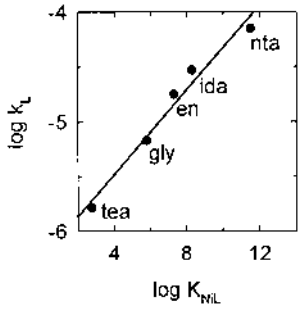

Fig. 8. LGER plot for the first-order dissolution rate constant and the stability constant in solution, for a series of Ni(II) complexes (redrawn from Refs. [135,136]).

the electronic configuration of the central metal ion. Very well documented cases of large increases in the lability include the transformations Fe(III) → Fe(II) [140–146], Cr(III) → Cr(VI) [147,148], Cr(III) → Cr(II) [70], and Mn(IV) → Mn(II) [149,150]. Important effects are also produced by oxidants in the dissolution of UO_2, NiO and ZnO; on this subject, the reader may consult Ref. [127] and references therein. In redox dissolution, the reactive surface complex is created by a charge-transfer reaction, in which an oxidizing or reducing agent from the solution reacts with the metal center. The resulting surface complex may in fact be highly reactive, and it reaches only a low steady-state concentration [131]. In general, complexing agents are required to assist the redox reaction.

We shall briefly analyze the case of reductive dissolution of an oxide M_2O_3; other cases are not very different. Heterogeneous electron transfer can take place to a large extent only if some other charge-compensating process accompanies it, usually proton transfer. In the absence of dissolution, surface reduction of the oxide results; the simplest dissolution kinetic scheme is of the type:

$$\equiv M(III)–L + X^- + H^+ \rightarrow \equiv M(II)–LH + X^{\cdot};\ k_{et}^{f} \tag{44}$$

$$\equiv M(II)–LH + X^{\cdot} \rightarrow \equiv M(III) + X^- + H^+;\ k_{et}^{r} \tag{45}$$

$$\equiv M(II)–LH \rightarrow M(II)(aq);\ k_{pht} \tag{46}$$

The steady-state condition is then given by:

$$\{\equiv M(II)–LH\} = \frac{k_{et}^{f}\{\equiv M(III)–L\}[X^-][H^+]}{k_{et}^{r}\{\equiv M(II)–LH\}[X^{\cdot}] + k_{pht}} \tag{47}$$

and the rate of dissolution is:

$$R = k_{pht}\{\equiv M(II)–LH\} = k_{pht}k_{et}^{f}\,\frac{\{\equiv M(III)–L\}[X^-][H^+]}{k_{et}^{r}\{\equiv M(II)–LH\}[X^{\cdot}] + k_{ph}} \tag{48}$$

In fact, the rate laws are generally more complicated, because L, X^- and H^+ usually become available through ionic adsorption, described by an adequate modification of Langmuir's equation, or even by a Freundlich isotherm. For our purposes, it is interesting to analyze the electron-transfer reactions (Eqs. (44) and (45)). As written, Eq. (44) describes either inner- or outer-sphere electron exchange between ≡M(III)–L and X^-; in fact, there are well documented cases of inner-sphere reactions in which X^- is a non-metallic reductant (ascorbate, dithiomite [151,152], or a reducing metal ion (Fe(II), Cr(II)). Contentions for outer-sphere reactions are scarce, the best established case being the interaction of $V(dipc)_3^-$ with iron(III) oxides [153]. In some cases, L and X^- are identical: for example, oxalate, oligocarboxylates and mercaptocarboxylates reductively dissolve iron(III) oxides [141,144,145].

When the complexing anion is also the reductant, the reversibility of the charge transfer (LMCT) limits the rate of the following dissolution reaction. The usual reductants for Fe(III) in solution have been explored as potential reductants for iron(III) oxides. The list includes iodide and thiocyanate, in addition to the above mentioned ligands. In the latter case, reversible LMCT was documented by the

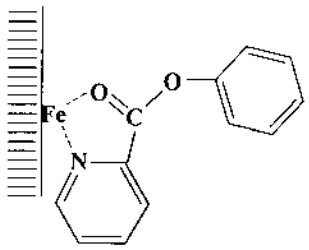

Fig. 9. Sketch of surface chelation by adsorbed phenyl isonicotinate. Redrawn from Ref. [167].

visible spectrum [98]; it was also shown that the rate of scavenging of $SCN^{\bullet}$ by SCN^{-} or other dissolved species limits the rate. The similarity with homogeneous redox chemistry is striking [154].

A particularly important and ubiquitous reductant is Fe(II) in the presence of adequate complexing agents (such as oligocarboxylates). The formation of mixed-valence surface complexes of the type ≡Fe(III)–L–Fe(II) is well demonstrated by the effect of Fe(II) on the rates of dissolution [141–143]. Coadsorption of Fe(II) and L produces the dimeric surface complex, and internal electron exchange facilitates the breakage of oxo bonds. The net result is the redox catalysis of dissolution in a stoichiometrically non-reductive reaction.

LMCT activation of ≡Fe(III)–L (L being an organic anion) by light absorption brings about dissolution [155–157]; this process, important in the iron cycling in aquatic chemistry [158], is similar to the well known photochemical decomposition of trisoxalatoferrate(III) and other iron(III)–carboxylate complexes [159].

5.3. Heterogeneous catalysis

Heterogeneous analogues to homogeneous metal ion catalysis are well known. Stone et al. have carried out a systematic study of ester hydrolysis catalysis by metals in the surface of various minerals [160–167]. Both carboxylate and phosphorothionate were studied, and several mechanisms of hydrolysis catalysis seem to operate in different cases. For this review, particularly relevant is the decrease of the half life of phenyl picolinate from 86 to 5 h, brought about by addition of TiO_2 or FeOOH. Phenyl isonicotinate hydrolysis rate is not affected, and it is concluded that a surface chelate, as depicted in Fig. 9, mediates the hydrolysis.

The presence of oxidant–reductant pairs on the surface of metal oxides is capable of producing an acceleration of the redox reaction. For example, α-FeOOH, γ-AlOOH and, more effectively TiO_2, catalyze the oxidation of a series of low molecular weight organic compounds by chromate(VI) [168,169]. It has been postulated that chromate is activated upon surface complexation, thus making it a stronger oxidant; alternatively, thermal activation may result from hole transfer to the valence band of the oxide (or to a localized state associated to the metal ion), followed by back transfer to the reductant. In fact, evidence of direct reduction of chromate on TiO_2, even in the absence of organic compounds was obtained recently by measurements of electrokinetic mobilities [170].

Redox catalysis is dramatically enhanced by shining light onto adequate substrates. Photocatalysis constitutes the basis of one of the advanced oxidation technologies for the destruction of pollutants in water. By far, the most promising method is based on titanium dioxide; Fig. 10 shows the basic processes involved.

The wealth of information on photocatalytic reactions is so large, that even a cursory review of the literature is outside the scope of this review. We shall however make a few comments about the role played by surface complexes. It is well known that there is no clear relationship between the rates of photooxidation and the extent of substrate adsorption. Several possibilities account for this fact: (a) reaction in solution phase, involving $OH^{\bullet}$ radicals and the substrate; (b) rate limitation by the availability of photons; and (c) rate limitation by recombination of e,h pairs. Recently we have shown however, that at least in one case, the oxidation of salicylate, an appropriate surface speciation accounts for the rate behavior [15]. Fig. 11 shows that the rate saturation is associated with the saturation of one of the three identified surface complexes, the one characterized by the largest stability constant (and lowest density of surface sites). Thus, the observed zero order on dissolved salicylate is simply due to constant surface concentration of the reactive complex.

The reaction of surface complexes with holes leads to oxidized species that easily evolve to organic free radicals. The evolution of these species depends on the interfacial dynamics; desorption, further charge transfer, or reaction with adsorbed oxidants all take place to a larger or lesser extent. Recently [171] we have demonstrated that under adequate conditions up to 28 valence-band holes and conduction-band electrons can be transferred to enact the total mineralization of salicylic acid:

$$C_7H_6O_3 + 11H_2O = 7CO_2 + 28H^+ + 28e^- \quad (49)$$

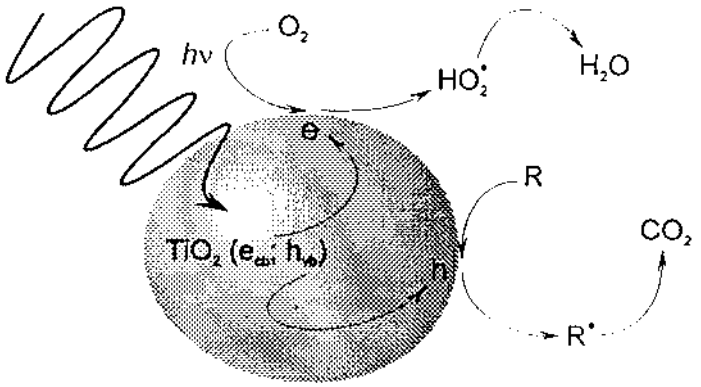

Fig. 10. Sketch representation of the photooxidation of dissolved organics catalyzed by dispersed TiO_2 particles.

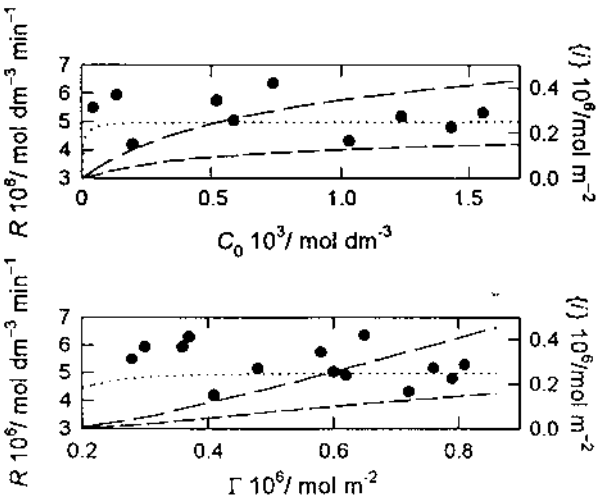

Fig. 11. Rates of the TiO_2-catalyzed photooxidation of salicylic acid at 299 K and pH 3.6 plotted as a function of the initial photolyte concentration (upper). The same information, including data at other pH values, is presented in the lower graph as a function of the salicylic acid surface excess. For comparison, the distribution of the different surface Ti(IV)-salicylate complexes is depicted by the lines: (– –) {*I*}; (— —) {*II*}; (···) {*III*}.

Acknowledgements

The work reported here has involved a large number of students and associates, as illustrated in the references. Work supported by CNEA, CONICET, ANPCYT, Fundación Antorchas, and CYTED. MAB, AER and PJM are members of CONICET. JAS and ADW acknowledge fellowships granted by CONICET. GEM acknowledges a leave of absence granted by U.N.Sur.

References

[1] H. Taube, H. Myers, J. Am. Chem. Soc. 76 (1954) 2103.
[2] M.A. Anderson, A.J. Rubin (Eds.), Adsorption of Inorganics at Solid-Liquid Interfaces, Ann Arbor Science, Ann Arbor, 1981.
[3] W. Stumm (Ed.), Aquatic Surface Chemistry, Wiley, New York, 1987.
[4] M.F. Hochella Jr., A.F. White (Eds.), Mineral-Water Interface Geochemistry, Rev. Mineralogy, 23, Mineralogical Society of America, Washington, DC, 1990.
[5] M.A. Blesa, P.J. Morando, A.E. Regazzoni, Chemical Dissolution of Metal Oxides, CRC Press, Boca Raton, FL, 1994.
[6] G.A. Parks, P.L. de Bruyn, J. Phys. Chem. 66 (1962) 967.
[7] J. Goniakowski, M.J. Gillan, Surf. Sci. 350 (1996) 145.
[8] R.L. Kurtz, R. Stockbauer, T.E. Madey, E. Román, J.L. de Segovia, Surf. Sci. 218 (1989) 178.
[9] M.A. Anderson, Surf. Sci. 355 (1996) 151.
[10] L.Q. Wang, D.R. Baer, M.H. Engelhard, A.N. Shultz, Surf. Sci. 344 (1995) 237.
[11] R. Iler, The Chemistry of Silica, Wiley, New York, 1979.

[12] A.C. Lasaga, in: M.F. Hochella Jr., A.F. White (Eds.), Mineral-Water Interface Geochemistry, Rev. Mineralogy, 23, Mineralogical Society of America, Washington, DC, 1990, p. 17.
[13] R.L. Parfitt, J.D. Russell, V.C. Farmer, J. Chem. Soc. Faraday Trans. I 72 (1976) 1082.
[14] R. Rodríguez, A.E. Regazzoni, M.A. Blesa, J. Colloid Interface Sci. 177 (1996) 122.
[15] A.E. Regazzoni, P. Mandelbaum, M. Matsuyoshi, S. Schiller, S.A. Bilmes, M.A. Blesa, Langmuir 14 (1998) 868.
[16] T. Hiemstra, W.H. van Riemsdijk, G.H. Bolt, J. Colloid Interface Sci. 133 (1989) 91.
[17] T. Hiemstra, J.C.M. de Wit, W.H. van Riemsdijk, J. Colloid Interface Sci. 133 (1989) 105.
[18] T. Hiemstra, W.H. van Riemsdijk, Colloids Surf. 59 (1991) 7.
[19] T. Hiemstra, P. Vanema, W.H. van Riemsdijk, J. Colloid Interface Sci. 184 (1996) 680.
[20] M.A. Blesa, A.J.G. Maroto, A.E. Regazzoni, J. Colloid Interface Sci. 140 (1990) 287.
[21] L.G.J. Fokkink, A. de Keizer, J. Lyklema, J. Colloid Interface Sci. 127 (1989) 116.
[22] D.A. Sverjensky, Geochim. Cosmochim. Acta 58 (1994) 3123.
[23] M.A. Blesa, G. Magaz, J.A. Salfity, A.D. Weisz, Solid State Ionics 101 (1997) 1235.
[24] G.E. Magaz, L.A. García Rodenas, P.J. Morando, M.A. Blesa, Croat. Chem. Acta 71 (1998) 917.
[25] A.E. Regazzoni, M.A. Blesa, A.J.G. Maroto, J. Colloid Interface Sci. 91 (1983) 560.
[26] P.W. Schindler, in: W. Stumm (Ed.), Aquatic Surface Chemistry, Wiley, New York, 1987, p. 83.
[27] P.H. Tewari, A.W. McLean, J. Colloid Interface Sci. 40 (1972) 267.
[28] K. Pulfer, P.W. Schindler, J.C. Westall, R. Graver, J. Colloid Interface Sci. 101 (1984) 554.
[29] A.E. Regazzoni, M.A. Blesa, A.J.G. Maroto, J. Colloid Interface Sci. 122 (1988) 315.
[30] P.H. Tewari, A.B. Campbell, J. Colloid Interface Sci. 55 (1976) 531.
[31] C.F. Baes, R. Mesmer, The Hydrolysis of Cations, Wiley, New York, 1970.
[32] P.R. Grossl, M. Eick, D.L. Sparks, S. Goldberg, C.C. Ainsworth, Environ. Sci. Technol. 31 (1997) 321.
[33] C.M. Eggleston, S. Hug, W. Stumm, B. Sulzberger, M. Dos Santos Afonso, Geochim. Cosmochim. Acta 62 (1998) 585.
[34] J.A. Davis, D.B. Kent, in: M.F. Hochella Jr., A.F. White (Eds.), Mineral-Water Interface Geochemistry, Rev. Mineralogy, 23, Mineralogical Society of America, Washington, DC, 1990, p. 177.
[35] J.A. Davis, J.O. Leckie, J. Colloid Interface Sci. 74 (1980) 32.
[36] C.H. Weng, J.H. Wang, C.P. Huang, Water Sci. Technol. 35 (1997) 55.
[37] N.W. Duffy, K.D. Dobson, K.C. Gordon, B.H. Robinson, A.J. McQuillan, Chem. Phys. Lett. 266 (1997) 451.
[38] B. Nowack, L. Sigg, J. Colloid Interface Sci. 177 (1996) 106.
[39] J. Rubio, E. Matijevič, J. Colloid Interface Sci. 68 (1979) 408.
[40] N. Kallay, E. Matijevič, Langmuir 1 (1985) 195.
[41] R. Torres, N. Kallay, E. Matijevič, Langmuir 4 (1988) 706.
[42] M.A. Blesa, E.B. Borghi, A.J.G. Maroto, A.E. Regazzoni, J. Colloid Interface Sci. 98 (1984) 295.
[43] D.A. Dzombak, F.M.M. Morel, Surface Complexation Modeling: Hydrous Ferric Oxide, Wiley-Interscience, New York, 1990, p. 306.
[44] R.S. Ramakrishna, V. Paramasigamani, M. Mahendran, Talanta 22 (1975) 523.
[45] B.A. Borgias, S.R. Cooper, Y.B. Koh, D.N. Raymond, Inorg. Chem. 23 (1984) 1009.
[46] D. Vasudevan, A.T. Stone, Environ. Sci. Technol. 30 (1996) 1604.
[47] D. Vasudevan, A.T. Stone, J. Colloid Interface Sci. 202 (1998) 1.
[48] A.T. Stone, A. Torrents, J. Smolen, D. Vasudevan, J. Hadley, Environ. Sci. Technol. 27 (1993) 895.
[49] G.E. Brown Jr., in: M.F. Hochella Jr., A.F. White (Eds.), Mineral-Water Interface Geochemistry, Rev. Mineralogy, 23, Mineralogical Society of America, Washington, DC, 1990, p. 309.
[50] M.I. Tejedor-Tejedor, M.A. Anderson, Langmuir 6 (1990) 602.
[51] S.J. Hug, J. Colloid Interface Sci. 188 (1997) 415.
[52] L.J. Turner, J.R. Kramer, Soil Sci. 152 (1991) 226.
[53] P. Persson, L. Lövgren, Geochim. Cosmochim. Acta 60 (1996) 2789.
[54] R.L. Parfitt, R. St. C. Smart, J. Chem. Soc. Faraday I 74 (1977) 796.
[55] R.L. Parfitt, R. St. C. Smart, Soil Sci. Soc. Am. J. 42 (1978) 48.

[56] C.J. Serna, J.L. White, S.L. Hem, Soil Sci. Soc. Am. J. 41 (1977) 1009.
[57] P. Persson, N. Nilsson, S. Sjöberg, J. Colloid Interface Sci. 177 (1996) 263.
[58] R.J. Atkinson, R.L. Parfitt, R. St. C. Smart, J. Chem. Soc. Faraday Trans. I 72 (1976) 1082.
[59] B. Barja, M.I. Tejedor-Tejedor, M.A. Anderson, Langmuir, submitted for publication.
[60] P. Persson, E. Laiti, L.O. Ohman, J. Colloid Interface Sci. 190 (1997) 341.
[61] R.L. Parfitt, J.D. Russell, J. Soil Sci. 28 (1977) 297.
[62] J.D. Russell, E. Paterson, A.R. Fraser, V.C. Farmer, J. Chem. Soc. Faraday Trans. I 71 (1975) 1623.
[63] W.A. Zeltner, M.A. Anderson, Langmuir 4 (1988) 469.
[64] K.D. Dobson, J.A. McQuillan, Langmuir 13 (1997) 3392.
[65] X. Sun, H.E. Doner, Soil Sci. 161 (1996) 865.
[66] T.H. Hsia, S.L. Lo, C.F. Lin, D.Y. Lee, Colloids Surf. A 85 (1994) 1.
[67] R.L. Parfitt, V.C. Farmer, J.D. Russell, J. Soil Sci. 28 (1977) 29.
[68] R.L. Parfitt, A.R. Fraser, J.D. Russell, V.C. Farmer, J. Soil Sci. 28 (1977) 40.
[69] S.J. Hug, B. Sulzberger, Langmuir 10 (1994) 3587.
[70] L.A. García Rodenas, A.M. Iglesias, A.D. Weisz, P.J. Morando, M.A. Blesa, Inorg. Chem. 36 (1997) 6423.
[71] A.D. Weisz, M.A. Blesa, work in progress.
[72] R.M. Cornell, P.W. Schindler, Colloid Polym. Sci. 258 (1980) 1171.
[73] P.A. Connor, K.D. Dobson, A.J. McQuillan, Langmuir 11 (1995) 4193.
[74] M.I. Tejedor-Tejedor, E.C. Yost, M.A. Anderson, Langmuir 6 (1990) 979.
[75] S. Tunesi, M.A. Anderson, Langmuir 8 (1992) 487.
[76] M.I. Tejedor-Tejedor, E.C. Yost, M.A. Anderson, Langmuir 8 (1992) 525.
[77] N. Nilsson, P. Persson, L. Lövgren, S. Sjöberg, Geochim. Cosmochim. Acta 60 (1996) 4385.
[78] B. Gu, J. Schmitt, Z. Chen, L. Liang, J.F. McCarthy, Geochim. Cosmochim. Acta 59 (1995) 219.
[79] K.H. Kung, M.B. McBride, Clays Clay Miner. 37 (1989) 333.
[80] K.H. Kung, M.B. McBride, Soil Sci. Soc. Am. J. 53 (1989) 1673.
[81] E.C. Yost, M.I. Tejedor-Tejedor, M.A. Anderson, Environ. Sci. Technol. 24 (1990) 822.
[82] W.A. Zeltner, E.C. Yost, M.L. Machesky, M.I. Tejedor-Tejedor, M.A. Anderson, in: J.A. Davis, K.F. Hayes (Eds.), Geochemical Processes at Mineral Surfaces, American Chemical Society, Washington, DC, 1986, p. 142.
[83] M.V. Biber, W. Stumm, Environ. Sci. Technol. 28 (1994) 763.
[84] J.D. Kubicki, M.J. Itoh, L.M. Schroeter, S.E. Apitz, Environ. Sci. Technol. 31 (1997) 1151.
[85] K.H. Kung, M.B. McBride, Environ. Sci. Technol. 25 (1991) 702.
[86] M.B. McBride, K.H. Kung, Environ. Toxicol. Chem. 10 (1991) 441.
[87] M.B. McBride, L.G. Wesselink, Environ. Sci. Technol. 22 (1988) 703.
[88] S.T. Martin, J.M. Kesselman, D.S. Park, N.S. Lewis, M.R. Hoffmann, Environ. Sci. Technol. 30 (1996) 2535.
[89] P. Falaras, M. Graetzel, A. Hugotlegoff, M. Nazeeruddin, E. Vrachnou, J. Electrochem. Soc. 140 (1993) L92.
[90] F. Heinz, D.J. Fitzmaurice, M. Graetzel, Langmuir 6 (1990) 198.
[91] B.A. Holmén, M.I. Tejedor-Tejedor, W.H. Casey, Langmuir 13 (1997) 2197.
[92] A. Couzis, E. Gulari, Langmuir 9 (1993) 3414.
[93] A.S. Peck, L.H. Raby, M.E. Wadsworth, Trans. Soc. Miner. Eng. AIME 235 (1966) 301.
[94] C. Gutiérrez, Int. J. Miner. Process. 3 (1976) 247.
[95] K.K. Singh, P.R. Sarode, P. Ganguly, J. Chem. Soc. Dalton Trans. (1983) 1895.
[96] P. Ratnasamy, A.J. Leonard, J. Phys. Chem. 76 (1972) 1838.
[97] M.J. Schmelz, T. Miyasaua, S. Mizushima, T.J. Lane, J.V. Quagliano, Spectrochim. Acta 9 (1957) 51.
[98] A.E. Regazzoni, M.A. Blesa, Langmuir 7 (1991) 473.
[99] P.V. Kamat, Langmuir 1 (1985) 608.
[100] C.C. Ainsworth, D.M. Friedrich, P.L. Gassman, Z. Wang, A.B. Joly, Geochim. Cosmochim. Acta 62 (1998) 595.
[101] J. Moser, S. Punchihewa, P.P. Infelta, M. Graetzel, Langmuir 7 (1991) 3012.

[102] J.G. Hering, W. Stumm, Langmuir 7 (1991) 1567.
[103] V.H. Houlding, M. Graetzel, J. Am. Chem. Soc. 105 (1983) 5695.
[104] P.V. Kamat, M.A. Fox, Chem. Phys. Lett. 102 (1983) 379.
[105] J. Moser, M. Graetzel, J. Am. Chem. Soc. 106 (1984) 6557.
[106] M.A. Ryan, E.C. Fitzgerald, M.T. Spitler, J. Phys. Chem. 93 (1989) 6150.
[107] H. Frei, D.J. Fitzmaurice, M. Gratzel, Langmuir 6 (1990) 198.
[108] P.V. Kamat, J. Photochem. 28 (1985) 513.
[109] K.R. Gopidas, P.V. Kamat, Mol. Cryst. Liq. Cryst. 183 (1990) 403.
[110] K. Chandrasenkaran, J.K. Thomas, J. Am. Chem. Soc. 105 (1983) 6383.
[111] P.V. Kamat, K.R. Gopidas, D. Weir, Chem. Phys. Lett. 149 (1988) 491.
[112] P.V. Kamat, W.E. Ford, Chem. Phys. Lett. 135 (1987) 421.
[113] K.R. Gopidas, P.V. Kamat, J. Phys. Chem. 93 (1989) 6428.
[114] M.T. Spitler, M.J. Calvin, J. Chem. Phys. 66 (1977) 4294.
[115] K. Hashimoto, M. Hiramoto, T. Sakata, J. Phys. Chem. 92 (1988) 4272.
[116] A. Kay, R.H. Baker, M. Graetzel, J. Phys. Chem. 98 (1994) 952.
[117] K.W. Weissmahr, S.B. Haderlein, R.P. Schwarzenbach, Environ. Sci. Technol. 31 (1997) 240.
[118] S. Fendorf, M.J. Eick, P. Grossl, D.L. Sparks, Environ. Sci. Technol. 31 (1997) 315.
[119] A. Manceau, L. Charlet, J. Colloid Interface Sci. 168 (1994) 87.
[120] K.F. Hayes, A.L. Roe, G.E. Brown Jr., K.O. Hodgson, J.O. Leckie, G.A. Parks, Science 238 (1987) 783.
[121] C. Papelis, G.E. Brown Jr., G.A. Parks, J.O. Leckie, Langmuir 11 (1996) 2041.
[122] A. Manceau, Geochim. Cosmochim. Acta 59 (1995) 3647.
[123] G.A. Waychunas, C.C. Fuller, B.A. Rea, J.A. Davis, Geochim. Cosmochim. Acta 60 (1996) 1765.
[124] G.A. Waychunas, B.A. Rea, C.C. Fuller, J.A. Davis, Geochim. Cosmochim. Acta 57 (1993) 2251.
[125] B.A. Manning, S.E. Fendorf, S. Goldberg, Environ. Sci. Technol. 32 (1998) 2383.
[126] M.L. Peterson, G.E. Brown Jr., G.A. Parks, Colloids Surf. A 107 (1996) 77.
[127] M.A. Blesa, P.J. Morando, A.E. Regazzoni, Chemical Dissolution of Metal Oxides, CRC Press, Boca Raton, 1994, Ch. 9.
[128] E. Wieland, B. Wehrli, W. Stumm, Geochim. Cosmochim. Acta 52 (1988) 1969.
[129] C. Lüdwig, W.H. Casey, J. Colloid Interface Sci. 178 (1996) 176.
[130] V.I.E. Bruyère, M.A. Blesa, J. Electroanal. Chem. 182 (1985) 141.
[131] V.I.E. Bruyère, P.J. Morando, M.A. Blesa, J. Colloid Interface Sci. 209 (1999) 207.
[132] G. Sposito, The Surface Chemistry of Soils, Oxford University Press, New York, 1984, p. 85.
[133] G. Sposito, Environ. Sci. Technol. 32 (1998) 2815.
[134] W.H. Casey, C. Lüdwig, in: A.F. White, S.L. Brantley (Eds.), Chemical Weathering Rates in Silicate Minerals, Rev. Mineralogy, 31, Mineralogical Society of America, Washington, DC, 1995, p. 87.
[135] C. Lüdwig, W.H. Casey, P.A. Rock, Nature 375 (1995) 44.
[136] C. Lüdwig, J. Devidal, W.H. Casey, Geochim. Cosmochim. Acta 60 (1996) 213.
[137] G. Furrer, W. Stumm, Geochim. Cosmochim. Acta 50 (1986) 1847.
[138] For a discussion, see p. 353 in M.A. Blesa, P.J. Morando, A.E. Regazzoni, Chemical Dissolution of Metal Oxides, CRC Press, Boca Raton, 1994.
[139] E.C. Baumgartner, M. Litter, J. Romagnolo, M.A. Blesa, J. Chem. Soc. Faraday Trans. I 94 (1998) 115.
[140] M.A. Blesa, H.A. Marinovich, E.C. Baumgartner, A.J.G. Maroto, J. Chem. Soc. Faraday Trans. I 84 (1987) 3713.
[141] M. del V. Hidalgo, N.E. Katz, A.J.G. Maroto, M.A. Blesa, J. Chem. Soc. Faraday Trans. I 84 (1988) 199.
[142] M. del V. Hidalgo, N.E. Katz, A.J.G. Maroto, M.A. Blesa, J. Chem. Soc. Faraday Trans. I 84 (1988) 9.
[143] E.B. Borghi, A.E. Regazzoni, A.J.G. Maroto, M.A. Blesa, J. Colloid Interface Sci. 130 (1989) 199.
[144] E.B. Borghi, P.J. Morando, M.A. Blesa, Langmuir 7 (1991) 1652.
[145] E.B. Borghi, S.P. Alí, P.J. Morando, M.A. Blesa, J. Nucl. Mater. 229 (1996) 115.
[146] A. Amirbahman, L. Sigg, V.J. von Gunten, J. Colloid Interface Sci. 194 (1997) 194.

[147] G.B. Reartes, P.J. Morando, M.A. Blesa, Chem. Mater. 3 (1991) 1101.
[148] L. García Rodenas, M. Chocrón, P.J. Morando, M.A. Blesa, Can. J. Chem. 74 (1996) 103.
[149] A.T. Stone, J.J. Morgan, Environ. Sci. Technol. 18 (1984) 617.
[150] A.T. Stone, Environ. Sci. Technol. 21 (1987) 979.
[151] M. dos Santos Afonso, P.J. Morando, M.A. Blesa, S. Banwart, W. Stumm, J. Colloid Interface Sci. 138 (1990) 74.
[152] E.H. Rueda, M.C. Ballesteros, R.L. Grassi, M.A. Blesa, Clays Clay Miner. 40 (1992) 575.
[153] M.G. Segall, R.M. Sellers, J. Chem. Soc. Chem. Commun. (1980) 991.
[154] S.P. Alí, M.A. Blesa, P.J. Morando, A.E. Regazzoni, Langmuir 12 (1996) 4934.
[155] M.I. Litter, M.A. Blesa, J. Colloid Interface Sci. 125 (1988) 679.
[156] M.I. Litter, M.A. Blesa, Can. J. Chem. 68 (1990) 728.
[157] M.I. Litter, M.A. Blesa, Can. J. Chem. 70 (1992) 2502.
[158] M.I. Litter, E.C. Baumgartner, G.A. Urrutia, Environ. Sci. Technol. 25 (1991) 1907.
[159] J.H. Baxendale, N.K. Bridge, J. Phys. Chem. 59 (1955) 783.
[160] A.T. Stone, J. Colloid Interface Sci. 127 (1989) 429.
[161] A. Torrents, A.T. Stone, Environ. Sci. Technol. 25 (1991) 143.
[162] A. Torrents, A.T. Stone, Environ. Sci. Technol. 27 (1993) 1060.
[163] A. Torrents, A.T. Stone, J. Soil Sci. Soc. Am. 58 (1994) 738.
[164] A.T. Stone, A. Torrents, in: P.M. Huang (Ed.), Environmental Impact of Soil Components Interactions, Lewis, Chelsea, MI, 1995.
[165] J.M. Smolen, A.T. Stone, Environ. Sci. Technol. 31 (1997) 164.
[166] J.M. Smolen, A.T. Stone, J. Soil Sci. Soc. Am. 62 (1998) 636.
[167] A.T. Stone, in: D.L. Macalady (Ed.), Perspectives in Environmental Chemistry, Oxford University Press, New York, 1998, Ch. 4.
[168] B. Deng, A.T. Stone, Environ. Sci. Technol. 30 (1996) 463.
[169] B. Deng, A.T. Stone, Environ. Sci. Technol. 30 (1996) 2484.
[170] G. Magaz, A.D. Weisz, L. García Rodenas, M.A. Blesa, I Jorn. Arg. Qca. Inorg. La Plata, 1998.
[171] P. Mandelbaum, S.A. Bilmes, A.E. Regazzoni, M.A. Blesa, Solar Energy, in press.